doi:10.1093/brain/awv227 BRAIN 2015: 138; 2875–2890 | 2875

BRAIN
A JOURNAL OF NEUROLOGY

GABAergic inhibition shapes interictal dynamics in awake epileptic mice

Sarah Feldt Muldoon,[1,2,3,*,†] Vincent Villette,[1,2,3,*] Thomas Tressard,[1,2,3] Arnaud Malvache,[1,2,3] Susanne Reichinnek,[1,2,3] Fabrice Bartolomei[4] and Rosa Cossart[1,2,3]

*These authors contributed equally to this work.

Epilepsy is characterized by recurrent seizures and brief, synchronous bursts called interictal spikes that are present in-between seizures and observed as transient events in EEG signals. While GABAergic transmission is known to play an important role in shaping healthy brain activity, the role of inhibition in these pathological epileptic dynamics remains unclear. Examining the microcircuits that participate in interictal spikes is thus an important first step towards addressing this issue, as the function of these transient synchronizations in either promoting or prohibiting seizures is currently under debate. To identify the microcircuits recruited in spontaneous interictal spikes in the absence of any proconvulsive drug or anaesthetic agent, we combine a chronic model of epilepsy with *in vivo* two-photon calcium imaging and multiunit extracellular recordings to map cellular recruitment within large populations of CA1 neurons in mice free to run on a self-paced treadmill. We show that GABAergic neurons, as opposed to their glutamatergic counterparts, are preferentially recruited during spontaneous interictal activity in the CA1 region of the epileptic mouse hippocampus. Although the specific cellular dynamics of interictal spikes are found to be highly variable, they are consistently associated with the activation of GABAergic neurons, resulting in a perisomatic inhibitory restraint that reduces neuronal spiking in the principal cell layer. Given the role of GABAergic neurons in shaping brain activity during normal cognitive function, their aberrant unbalanced recruitment during these transient events could have important downstream effects with clinical implications.

1 Institut National de la Santé et de la Recherche Médicale Unité 901, 13009 Marseille, France
2 Aix-Marseille Université, Unité Mixte de Recherche S901, 13009 Marseille, France
3 Institut de Neurobiologie de la Méditerranée, 13009 Marseille, France
4 Institut des Neurosciences des Systèmes, Institut National de la Santé et de la Recherche Médicale Unité 1106, 13005 Marseille, France

†Present address: Department of Mathematics and Computational Data Science and Engineering Program, University at Buffalo, SUNY, Buffalo, NY 14260, USA

Correspondence to: Dr Rosa Cossart,
Institut de Neurobiologie de la Méditerranée,
INMED UMR901,
Parc Scientifique de Luminy BP 13,
13273 Marseille cedex 09,
France
E-mail: rosa.cossart@inserm.fr

Keywords: epilepsy; interictal spikes; calcium imaging; GABA; microcircuits

Abbreviations: kCSD = kernel current source density; TLE = temporal lobe epilepsy

Received December 17, 2014. Revised June 9, 2015. Accepted June 22, 2015. Advance Access publication August 13, 2015

Introduction

Interictal spikes are an electrophysiological marker of epilepsy (Gibbs *et al*., 1935) that occur much more frequently than seizures. These transient EEG signals are characterized by a short duration (<100 ms), large amplitude, and can be classified as multiphasic or single spikes (Huneau *et al*., 2013), which usually include a sharp spike followed by a slower wave. For clinical reasons, less significance is given to interictal spikes than to ictal events, as the former are not associated with any salient clinical manifestation. However, even in seizure-free patients, interictal spikes may lead to transitory cognitive impairment (Binnie, 2003) and episodic interictal memory disturbances (Mosbah *et al*., 2014). Furthermore, the function of these spikes is highly debated and has been proposed both as a protective phenomenon against the emergence of paroxysmal activities (de Curtis and Avanzini, 2001), or conversely, as a prelude to seizures (Staley *et al*., 2011). Similar to seizures, interictal spikes can originate from multiple foci and propagate to the surrounding regions through multiple paths (Chagnac-Amitai and Connors, 1989; Badier and Chauvel, 1995). In fact, in temporal lobe epilepsy (TLE), interictal spiking frequently originates from multiple subsets of temporal lobe structures, sometimes outside of the epileptogenic zone (Bourien *et al*., 2005).

The study of interictal spikes is therefore of special interest because, despite their association with epileptogenesis (Staley *et al*., 2011; Avoli *et al*., 2013; Huneau *et al*., 2013), their diagnostic yield (Blume *et al*., 2001), possible causal link to seizures (Avoli *et al*., 2013), and relationship to cognitive impairment, little is known about the specific microcircuits recruited throughout their propagation. Given the dual role of GABAergic circuits in dampening excitation and in coordinating the network oscillations that support cognitive function, it is therefore critical to specifically examine the spatio-temporal patterns of micro-scale inhibitory function.

One of the early identified possible roles of inhibition in epileptiform discharges was that of a restraint, or an 'inhibitory surround' that would function to oppose the spread of epileptic activity, thus creating an area of uncorrelated and sparsely propagating activity around the epileptogenic zone (Prince and Wilder, 1967). This phenomenon has been particularly well documented in human patients or drug-induced models of neocortical epilepsy in relation to ictal events (Prince and Wilder, 1967; Dichter and Spencer, 1969*a*, *b*; Trevelyan *et al*., 2006; Trevelyan, 2009; Sabolek *et al*., 2012; Schevon *et al*., 2012; Trevelyan and Schevon, 2013). Alternatively, it has been proposed that GABAergic transmission could initiate the synchronization process leading to paroxysmal discharges in the hippocampal formation of patients with drug-resistant TLE (Alvarado-Rojas *et al*., 2013). Although this debate has yet to be resolved, it is clear that the relation between interictal spiking and single-cell activity depends both on the type of epilepsy and the recording site, and is more heterogeneous than simple paroxysmal depolarization shifts (Prince and Wilder, 1967; Dichter and Spencer, 1969*a*, *b*; Trevelyan *et al*., 2006; Zhou *et al*., 2007; Trevelyan, 2009; Keller *et al*., 2010; Truccolo *et al*., 2011; Sabolek *et al*., 2012; Schevon *et al*., 2012; Alvarado-Rojas *et al*., 2013; Feldt Muldoon *et al*., 2013; Trevelyan and Schevon, 2013).

In TLE, the hippocampus is often linked to the site of seizure initiation, and here, epileptogenesis has been traditionally associated with GABAergic cell death and an overall dysfunction of inhibition. However, it is becoming increasingly clear that the diversity of GABAergic cell fates during epileptogenesis mirrors the morpho-functional heterogeneity of this cell population (Cossart *et al*., 2005). While some GABAergic microcircuits are selectively destroyed during epileptogenesis, those that are spared can be functionally (Chen *et al*., 2001; Cossart *et al*., 2001; Marchionni and Maccaferri, 2009) and/or anatomically (Nusser *et al*., 1997; Peng *et al*., 2013) boosted.

To fully understand the contribution of this modified inhibitory circuitry in shaping interictal dynamics, it is additionally important to study epileptic activity in the absence of anaesthetics. Recently, it has become clear that anaesthetics can modify neuronal activity, and firing rates and spike bursting have been shown to be higher, and correlated activity weaker, in awake compared to anaesthetized rats (Greenberg *et al*., 2008). Therefore, one must quantify the exact contribution of spatially distributed distinctive neurons to epileptiform dynamics under awake, *in vivo* conditions to fully understand how these diverse microcircuits contribute to pathological activity.

To this aim, we used a chronic model of TLE and studied spontaneous neuronal dynamics in the CA1 region of awake head restrained mice, free to run on a self-paced treadmill, using combined electrophysiological and two-photon calcium microscopy techniques. Although TLE mice displayed both interictal as well as ictal activity, we restricted our study to spontaneous interictal spikes, as the probability of observing a seizure was extremely low (see the Supplementary material for a discussion of seizure dynamics). Here, we focus our efforts on studying the spatial patterns of cellular recruitment during interictal spikes that propagate through the CA1 region of the hippocampus. CA1 is a very commonly studied region in the framework of epilepsy (Cossart *et al*., 2001; Bernard *et al*., 2004; Krook-Magnuson *et al*., 2013) and, through a dysregulated temporoammonic pathway, serves as an entry point into the hippocampus that enables the propagation of epileptiform activity directly from the entorhinal cortex, bypassing the classical trisynaptic loop (Wozny *et al*., 2005; Ang *et al*., 2006).

To isolate the recruitment of GABAergic microcircuits during interictal spikes, we additionally used a transgenic mouse line that allows for the restricted viral expression of a calcium reporter protein in only these cells (Tolu *et al*., 2010; Melzer *et al*., 2012). We found that during interictal

spikes, CA1 inhibition is synchronized, which leads to the quieting of neurons in the pyramidal cell layer. Therefore, we identify a dysfunction of the CA1 feedforward inhibitory microcircuit that potentially acts as an inhibitory brake to the propagation of epileptiform dynamics from the hippocampus to the rest of the brain (Prince and Wilder, 1967; Dichter and Spencer, 1969*a*, *b*; Trevelyan *et al.*, 2006; Trevelyan, 2009; Sabolek *et al.*, 2012; Schevon *et al.*, 2012; Trevelyan and Schevon, 2013), and contributes to a functional deafferentation of the subiculum (Cohen *et al.*, 2002; Wozny *et al.*, 2003), even in the absence of hippocampal sclerosis. This finding challenges the intuitive view that epilepsy results from an imbalance of inhibitory and excitatory action in favour of runaway excitation and instead supports earlier work (Prince, 1968; Velazquez and Carlen, 1999; Cohen *et al.*, 2002; Klaassen *et al.*, 2006; Zhou *et al.*, 2007; Marchionni and Maccaferri, 2009; Avoli and de Curtis, 2011; Huberfeld *et al.*, 2011) as well as theoretical predictions (Li *et al.*, 2008) indicating that the GABAergic microcircuits that are spared in the course of epileptogenesis contribute in shaping interictal discharges.

Materials and methods

Here we present a condensed version of the experimental and analytical methods. For complete descriptions, please see the Supplementary material. All protocols were performed under the guidelines of the French National Ethic Committee for Sciences and Health report on 'Ethical Principles for Animal Experimentation' in agreement with the European Community Directive 86/609/EEC under agreement #01413.03. Unless otherwise noted, all analysis was carried out in MATLAB using custom-made code, which can be provided by the authors upon request. Error bars denote standard error of the mean (SEM), and when necessary, Kolmogorov-Smirnov tests were used to assess the normality of distributions. Sample sizes were chosen to ensure experimental reproducibility and robustness while minimizing animal distress.

The pilocarpine model of temporal lobe epilepsy

Male adult wild-type Swiss mice ($n = 14$) or GAD67-Cre mice (Tolu *et al.*, 2010; Melzer *et al.*, 2012) ($n = 4$) crossed onto a Swiss background were used for experiments. As previously described (Feldt Muldoon *et al.*, 2013), mice were subjected to the pilocarpine model of TLE (Cavalheiro *et al.*, 1996). To ensure that the mice had reached the chronic phase of the model (displayed both interictal spikes and seizures), we waited an average of 58 ± 11 days (range 26–136) between pilocarpine injections and the first recording session (Supplementary Fig. 1A).

Interictal spike detection

To detect the occurrence of spontaneous interictal spikes, mice were implanted contralaterally with a global cortico-hippocampal electroencephalogram (contralateral EEG), hippocampal local field potential (contralateral LFP) and neck electromyogram (EMG) as shown in Fig. 1A. Interictal spikes were semi-automatically detected from the electrophysiological data simultaneously recorded in the contralateral hemisphere during imaging/probe recording sessions using custom-made software written in MATLAB. First, to remove noise artefacts, contralateral EEG and contralateral local field potential signals were filtered between 1 and 25 Hz using a fourth order Butterworth filter, and a threshold value was calculated using a moving standard deviation of the filtered signal over a 5-s sliding window (Supplementary Fig. 1B). Potential spikes were selected as points where both the filtered contralateral EEG and contralateral local field potential signals exceed this threshold. Potential spikes were then visually compared to the EMG signal to separate true spikes from movement artefacts, and the start and end times of the spike were manually marked using the unfiltered signal.

Linear probe recordings

A 16-channel linear silicon probe was used to obtain acute recordings of the LFP depth profile of the CA1 region in TLE mice ($n = 4$ mice). The spatial properties describing sinks and sources during interictal spikes were evaluated using the 13 channel LFPs from these linear probe recordings and a kernel current source density method (kCSD, for further details see Potworowski *et al.*, 2012). In one mouse of the four used for the probe experiments, the recorded signal saturated the amplifier during the spikes so this mouse was discarded from the kCSD analysis. Additionally, in one other mouse, obvious movement artefacts occurred during seven interictal spikes so these spikes were also removed from the analysis. This resulted in a final analysis of $n = 158$ interictal spikes recorded from three mice. To analyse the multiunit activity of pyramidal cells, the probe channel in which unit activity could be seen visually was selected for multiunit detection. The signal was first zero phase digitally filtered between 300 and 3000 Hz using a fourth order Butterworth filter. A baseline movement-free period of 10 s was selected, and multiunit activity was detected as points in time where the signal exceeded a threshold of five times the standard deviation of the baseline signal. To compare firing rates before and after interictal spikes, the average firing rate was calculated for a 500-ms window immediately before and immediately after each spike. In one of the four mice used, we could not detect unit activity in any of the recorded channels and thus this mouse was discarded from further analysis, meaning that the analysis was performed over $n = 131$ interictal spikes recorded from three mice.

Calcium imaging

To perform large-scale calcium imaging, wild-type TLE mice were injected with a viral solution of either GCaMP5G ($n = 3$), GCaMP6m ($n = 3$), or TLE GAD67-Cre mice with a viral vector carrying a CRE-dependent version of GCaMP5G. This procedure induced the expression of the GCaMP indicator in all neurons within the field of view, as quantified using immunohistochemical analysis (Supplementary Fig. 2). To allow optical access to the hippocampus, a ~3-mm diameter craniotomy centred over injection sites was performed: the

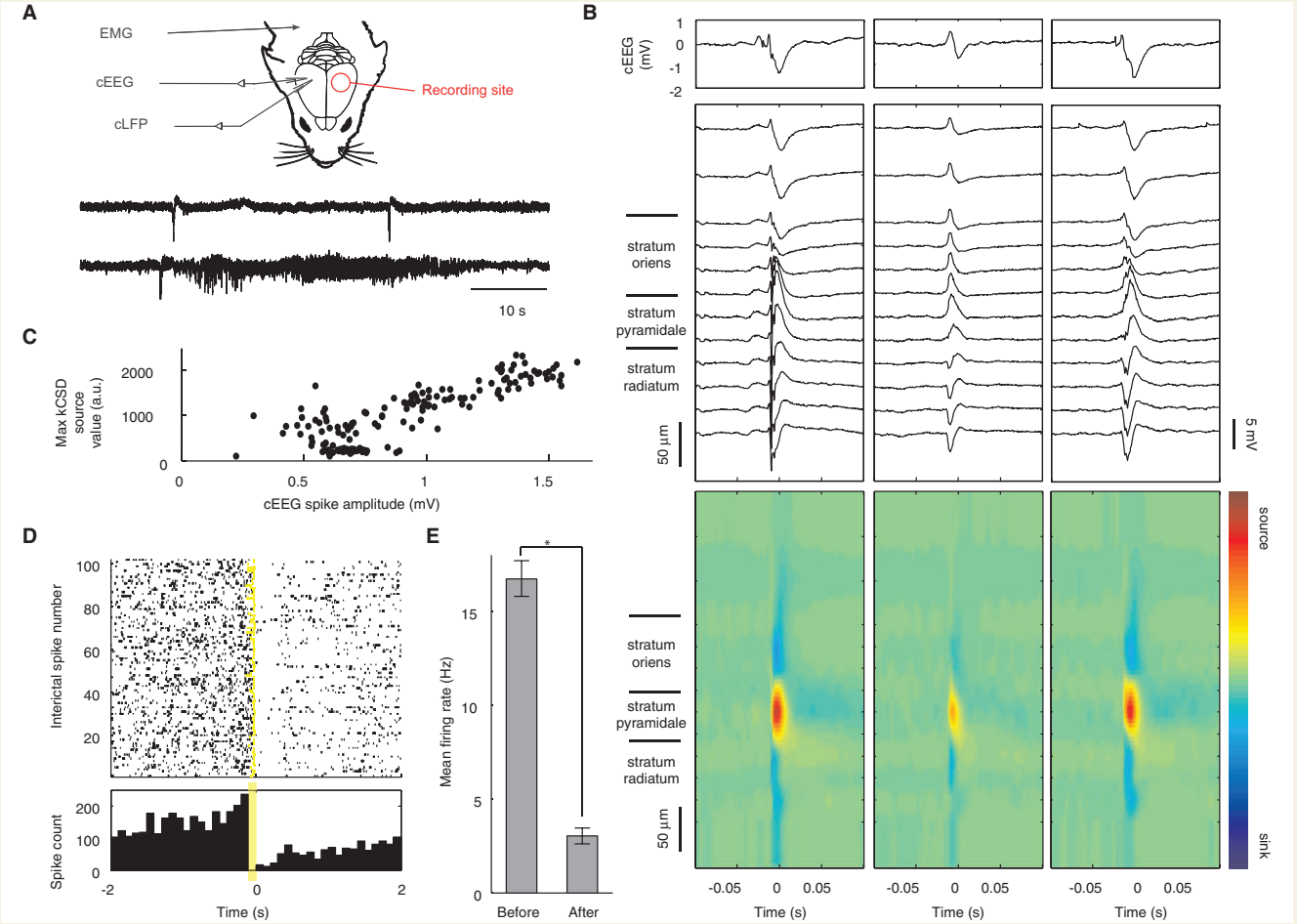

Figure 1 Electrophysiological properties of interictal spikes in CA1. (**A**) Schematic of chronic contralateral electrode placement and ipsilateral recording site (*upper*), contralateral EEG traces showing interictal spikes (*middle*) and ictal activity (lower). (**B**) Contralateral EEG (cEEG, *top*), linear probe recordings (*middle*), and corresponding kCSD analysis (*bottom*) for three interictal spikes from the same mouse. (**C**) Correlation between contralateral EEG and kCSD source amplitudes (Spearman's $\rho = 0.79$, $P < 0.001$, $n = 158$ interictal spikes from three mice). (**D**) Raster plot (*top*) and corresponding histogram (*bottom*) of multiunit activity in the stratum pyramidale for $n = 102$ interictal spikes from one mouse where $t = 0$ indicates spike time. Yellow boxes indicate time excluded due to the spike artefact. (**E**) Mean multiunit firing rate of stratum pyramidale cells 500 ms immediately before and after the spike (two-sample *t*-test, $P < 0.001$, $n = 131$ interictal spikes from three mice). Error bars represent SEM.

dura was gently cut and a small portion of the cortex was aspirated. A chronic glass window was implanted as previously reported (Dombeck *et al.*, 2010) but adapted slightly for large-scale imaging (Supplementary Fig. 1C). Although this procedure did involve the removal of a small portion of the cortex, the cortex was not removed for the linear probe recordings, and the spikes recorded on the contralateral EEG showed the same variability under both conditions. Additionally, all results are consistent between linear probe experiments and imaging experiments, so we conclude that our observations are not likely to be significantly affected by the surgical procedure.

All mice were handled before recording sessions to limit head restraint associated stress.

During imaging, mice were head-fixed on a non-motorized treadmill (adapted from Royer *et al.*, 2012) that allowed for self-paced locomotion to limit stress (Supplementary Fig. 1D). All experiments were performed in the dark. No rewards were given and the mice alternated between periods of moving and resting activity during recordings. The fluorescence activity from a 400 × 400 µm field of view (500 × 500 µm for × 20 objective) was acquired at ~7.7 Hz and recordings lasted ~4.5 min. Mice were imaged over multiple days (range 2–16 days). During imaging sessions, mice displayed spontaneous interictal spikes as detected in the contralateral EEG signal and these spike times were aligned with the corresponding movie frames through *post hoc* analysis.

For calibration experiments, mice ($n = 28$) were anaesthetized with ketamine (100 mg/kg) and xylazine (10 mg/kg) for surgery. A reference electrode was placed above the contralateral cerebellum and a glass coverslip with a hole allowing for pipette insertion covered hippocampal fibres. During recordings, a supplemental anaesthetic was provided if necessary (urethane, 1.5 g/kg, Sigma). Juxtacellular recordings were acquired using glass pipettes with a MultiClamp 700B Amplifier (Axon Instrument) and digitized at 20 kHz (Digidata1440a, Axon Instrument) while imaging as described above.

Spatial imprint analysis

To analyse the spatial patterning of cells recruited during interictal spikes, we calculated the 'spatial imprint' for each spike. Spatial imprints are composed of the pixel-by-pixel percentage change in fluorescence during a given interictal spike and therefore serve as a visual representation of the pixels activated during the spike. An image of baseline activity was created by averaging the movie frames acquired during a 500 ms window immediately preceding (but not including) the interictal spike (Supplementary Fig. 1E: 'Before image'). Similarly, an image representing the activity recorded during the spike was created by averaging the movie frames acquired during a 500-ms window immediately after (and including) the interictal spike (Supplementary Fig. 1E: 'After image'). We then produced the spatial imprint for each event by computing the dF/F image for the event, i.e. for each pixel, we calculated the change in fluorescence as (Image_after − Image_before) / Image_before. The spatial imprint is thus a normalized image that represents the spatial patterning of cell bodies and processes activated during each interictal spike, i.e. pixels that were active (experienced an increase in fluorescence) during the event appear brighter than those that were not active. In Supplementary Fig. 1E, the red arrow indicates a cell that did not participate in the spike, while the green arrow indicates a cell that was recruited during the spike.

Results

To identify the microcircuits recruited in spontaneous interictal spikes in the absence of any proconvulsive drug or anaesthetic agent, for the first time, we recorded electrical and optical signals from chronically epileptic awake mice using the pilocarpine model of TLE (Cavalheiro *et al.*, 1996). This widely used chronic model of epilepsy (Brooks-Kayal *et al.*, 1998; Cossart *et al.*, 2001; Smolders *et al.*, 2002; Fabene *et al.*, 2008; Hunt *et al.*, 2013) was chosen not only because spontaneous recurrent interictal spikes and seizures occur following an initial brain insult, but also because the development of such epileptiform activity has been associated with several well-described behavioural and structural network changes that reproduce the human pathology. Recordings from awake mice were achieved using head-restrained animals, allowed to self-regulate their motion on a non-motorized treadmill (Royer *et al.*, 2012). During each recording session, mice spontaneously alternated between run and rest periods, as their behaviour was not guided toward any reward.

Interictal spikes suppress multiunit activity in pyramidal cell layer

To observe epileptiform activities, TLE mice were chronically implanted with a contralateral macroscopic surface electroencephalogram (contralateral EEG), hippocampal CA1 local field potential (contralateral local field potential), and neck electromyogram (EMG) (Fig. 1A). Mice displayed spontaneous interictal spikes and seizures as observed in the contralateral EEG signal (Fig. 1A). Neuronal activity was then monitored ipsilaterally in the CA1 region of the hippocampus using either acute electrophysiological recordings with a linear silicone probe ($n = 171$ interictal spikes from four mice) or chronic two-photon calcium imaging ($n = 2619$ interictal spikes from 10 mice). The contralateral EEG signal was used for interictal spike detection, as these occurred simultaneously with local ipsilateral CA1 interictal spikes observed in linear probe recordings spanning the deeper neocortical layers down to the stratum radiatum (Supplementary Fig. 3). As previously described, interictal spikes are polymorphic events (Buzsaki *et al.*, 1991; Chauviere *et al.*, 2012) and all probe channels therefore expressed a wide heterogeneity in the interictal spike shape from event to event. However, kCSD analysis consistently revealed a source in the CA1 pyramidal cell layer (Fig. 1B). Interestingly, the strength of this local source was highly correlated with the amplitude of the global contralateral EEG spike (Fig. 1C, Spearman's $\rho = 0.79$, $n = 158$ interictal spikes from three mice). Although a source in the CA1 pyramidal layer is often produced by synchronous neuronal firing, it could also originate from a phasic perisomatic inhibitory input, and further information is needed to address this ambiguity (Buzsaki *et al.*, 2012). We therefore first examined multiunit activity in the CA1 pyramidal cell layer within a 2-s window centred on each interictal spike. Analysis revealed that multiunit frequency decreased immediately following interictal spikes, and this was consistently observed across all events in all animals (Fig. 1D and E, firing rate 500 ms before interictal spike = 16.7 ± 0.9 Hz, firing rate 500 ms after interictal spike = 3.0 ± 0.4 Hz, $n = 131$ interictal spikes from three mice). This striking result indicates that the kCSD source was likely due to pyramidal cells receiving a strong inhibition. Unfortunately, multiunit activity of pyramidal cells could not be assessed directly during the interictal spike due to the spike artefact (indicated by the yellow boxes in Fig. 1D), and we therefore turned to calcium imaging to further investigate cellular activity during the interictal spikes.

Calcium imaging of spontaneous interictal spikes

We used a viral vector to express the calcium reporter protein GCaMP5G ($n = 3$ mice) or GCaMP6m ($n = 3$ mice) in CA1 hippocampal cells (Akerboom *et al.*, 2012; Chen *et al.*, 2013). We adapted the surgical implantation of a previously described chronic window on the hippocampus that was shown to allow for the visualization of place cell firing (Dombeck *et al.*, 2010). This procedure allows for direct imaging of spontaneous activity in the stratum oriens (a layer with mostly somata of GABAergic neurons) and stratum pyramidale (mainly somata of glutamatergic principal cells) during interictal spikes over several days (range 2–16 days). All reported results were robust

throughout the entire imaging period. As with probe experiments, the detection of interictal spikes was based upon the contralateral EEG signal. During periods free of interictal spikes, cells were spontaneously active with more activity in the stratum pyramidale observed during periods of running, consistent with calcium imaging of non-epileptic, wild-type mice (Supplementary Fig. 4 and Supplementary Video 1).

In vivo two-photon imaging using GCaMP reporters has been previously used in the hippocampus to report bursting dynamics in place cells (Dombeck *et al.*, 2010) or to map neuronal activation during fear learning (Lovett-Barron *et al.*, 2014). However, it is important to understand if these reporters can reliably capture single-cell activation under conditions with lower neuronal firing rates. Although the GCaMP reporters have been shown to be sensitive to single action potential firing in the upper layers of the visual cortex *in vivo* (Chen *et al.*, 2013), it is unclear if these results hold under our conditions. As simultaneous imaging and patch-clamp recording is difficult under the hippocampal window, in order to probe the reliability of our experimental procedure for single action potential detection, we first tested whether we could detect the calcium transients associated with ripple events, a well-described physiological activity pattern that is known to produce single-spikes in CA1 pyramidal neurons within a similar time window as the interictal spikes (Csicsvari *et al.*, 1999; Gulyas and Freund, 2014). We detected ripple events in the contralateral local field potential of wild-type, non-epileptic mice ($n = 2$ mice) and observed time-locked calcium transients in stratum pyramidale neurons. These transients were of smaller amplitude than those associated with place-modulated firing, further indicating that they were produced by a few, if not single, spikes (Supplementary Fig. 5). In addition, using juxtacellular recordings from anaesthetized mice, we were able to record calcium signals in stratum pyramidale that aligned with the firing of action potentials and confirmed that sparse firing (approximately two to three spikes) produced significant calcium transients in these cells ($n = 4$ cells, Supplementary Fig. 6). Altogether, this indicates that our imaging set-up allows for the detection of single-cell activation during synchronous events, even when single-cell firing rate is low. Although the time resolution of the imaging does not allow for the evaluation of temporal sequences of cellular activation during these fast events, it instead provides information concerning the spatial patterning of cells that participate (or not) in events.

In both the stratum oriens and the stratum pyramidale, interictal spikes appeared as global flashes in the calcium movies (Fig. 2A and Supplementary Videos 2 and 3), indicating a large calcium rise throughout the CA1 region ($n = 1396$ interictal spikes from six mice). To examine the spatial patterning of cells involved in these spikes, we created a 'spatial imprint' of each interictal spike, i.e. an image that allows for the visualization of cell bodies and processes that were active during the event (Fig. 2B and C). In the spatial imprints of interictal spikes, we consistently observed a diffuse spatial patterning in the stratum pyramidale (Fig. 2B), compared to the clearly visible activation of somata and processes in the stratum oriens (Fig. 2C). Yet, when we pool all events (distributed throughout all observable imaging depths across both the stratum oriens and stratum pyramidale), we see a supralinear correlation between the amplitude of the spike recorded by the contralateral EEG and the amplitude of the fluorescence change associated with the interictal spike (Fig. 2D), with no dependence upon the depth of imaging. Thus the diffuse activation pattern observed in the stratum pyramidale followed the same relation as the spatially defined cellular activation patterns in the stratum oriens.

Differential recruitment of cells in stratum oriens versus pyramidale

To investigate further the relationship between firing of individual cells and the global calcium transient, we studied the dynamics of individual cells in both the stratum oriens and stratum pyramidale during interictal spikes using both the GCaMP5G and the more sensitive GCaMP6m variants of the reporter. Although one can see a faint increase in an individual cell's GCaMP signal during the interictal spike (Fig. 3A and B), cells show larger increase outside of events, indicating that cells with a soma in the stratum pyramidale are firing more when active outside of the interictal spike than during the spike. The same phenomenon was observed regardless of the indicator used (5G/6 m) so data from the two indicators were pooled for the remaining analysis.

To detect differences in neuronal recruitment during an interictal spike when imaging in the stratum oriens versus stratum pyramidale, we next compared the percentage of cells displaying a significant increase in the calcium signal (i.e. recruited cells) during large interictal spikes (i.e. interictal spikes with an average dF/F amplitude $>50\%$). Due to the differences in the density of cells between the stratum pyramidale and stratum oriens (Fig. 3D), we quantified the percentage of imaged cells that were recruited during interictal spikes, but absolute numbers of cells are also reported (Table 1). The percentage of neuronal recruitment in the stratum pyramidale was remarkably low (Fig. 3C, median = 0.6%), which represented a significantly lower fraction of cells than observed in the stratum oriens (Fig. 3C, median = 33%, two-sample Kolmogorov-Smirnov test, $P > 0.001$). This low percentage of active cells in the stratum pyramidale corresponds to, on average, 4 ± 1 cells (out of an estimated 766 ± 47 imaged cells in the stratum pyramidale) that are recruited during interictal spikes. On the contrary, in the stratum oriens, we see that a much higher fraction of cells are recruited (on average 2.1 ± 0.3 of a total of 7 ± 1 imaged cells), although this distribution is widespread and highly variable from event to event.

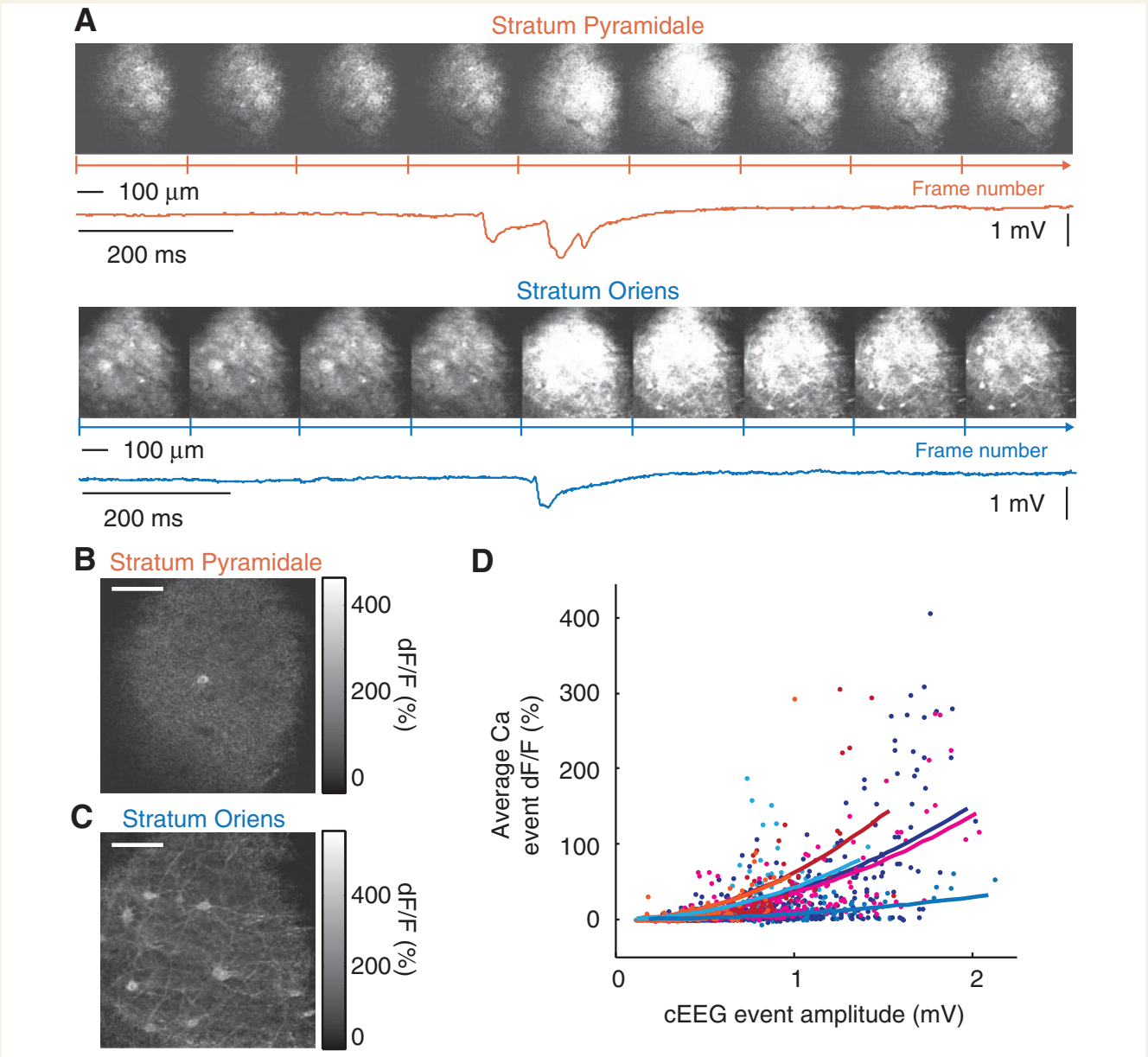

Figure 2 Calcium imaging of CA1. (**A**) Successive movie frames and simultaneous contralateral EEG signal for an interictal spike imaged in the stratum pyramidale (orange, Supplementary Video 2) or in the straum oriens (blue, Supplementary Video 3). (**B** and **C**) Corresponding spatial imprint during an interictal spike imaged in the stratum pyramidale (**B**) and stratum oriens (**C**). Scale bar represents 100 µm. (**D**) Relationship between the amplitude of the contralateral EEG and the average image dF/F during interictal spikes. Blue shades: GCaMP5 (n = 3 mice, 855 interictal spikes), red shades: GCaMP6 (n = 3 mice, 541 interictal spikes). Data from the stratum pyramidale and stratum oriens are pooled since the relationship was independent of the imaging location.

To further examine the sparse activation of cells in the stratum pyramidale, we additionally computed the number and percentage of cells that were active outside of interictal spikes (Table 1 and the Supplementary material). More pyramidal cells were active outside of interictal spikes (38 ± 10 cells) than during spikes (3.7 ± 0.7 cells). Even if the percentage of cells in the stratum pyramidale recruited during interictal spikes is calculated out of the number of cells that are active at some point outside of the spikes, the percentage of cells recruited during spikes rises only to an average value of $19.5 \pm 3.8\%$. Interestingly, as seen in the individual examples of cellular recruitment during interictal spikes, depicted in Fig. 3E, in the stratum pyramidale and stratum oriens, different subsets of cells are recruited in sequential events. Taken together, these results indicate that, while only subpopulations of cells participate in interictal spikes in both the stratum oriens and stratum pyramidale, the GABAergic cells located in the stratum oriens are more likely to be recruited during events. Given the lack of

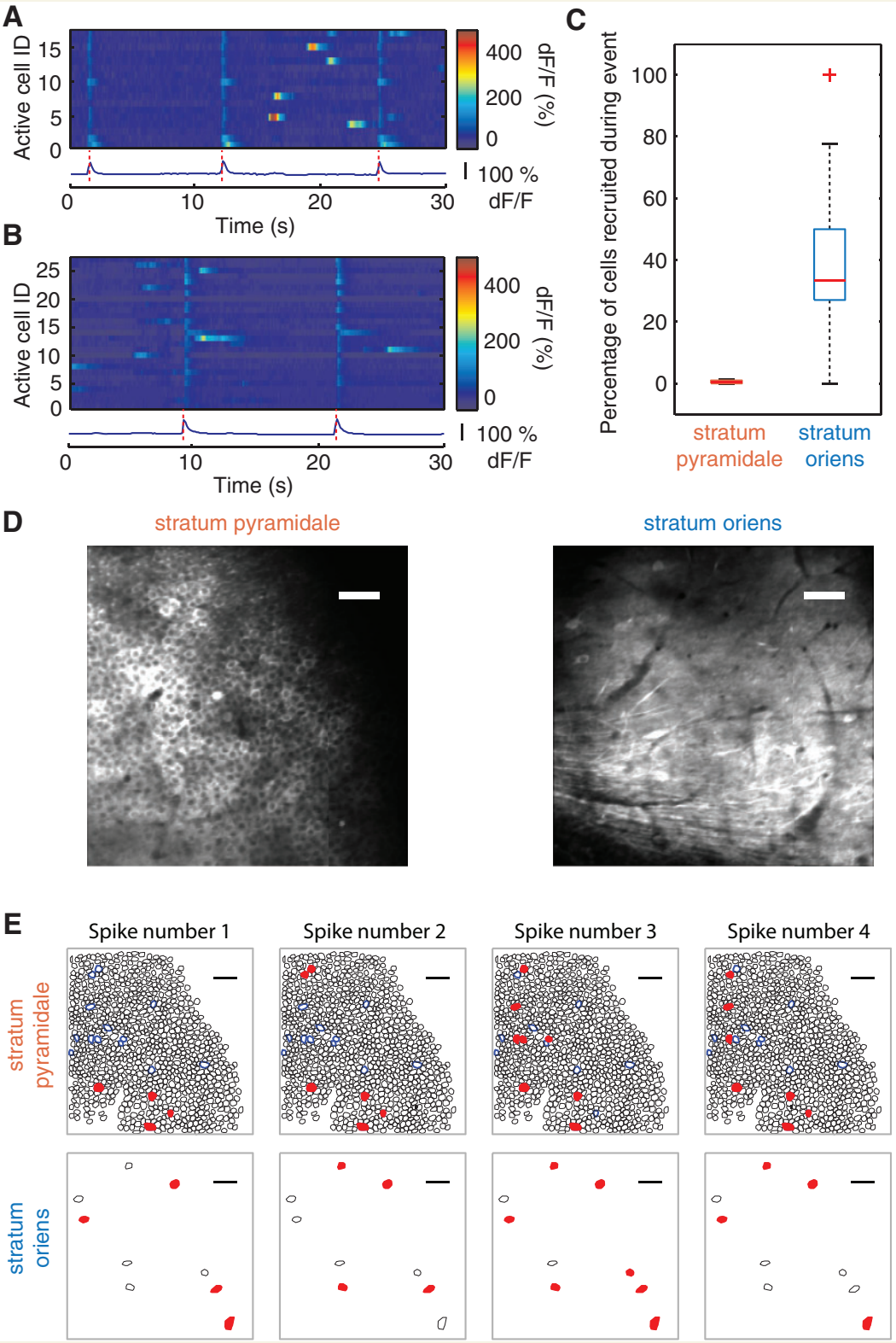

Figure 3 Single-cell participation in interictal spikes. (**A**) GCaMP5 signal from active cells (*top*) and corresponding dF/F averaged over the entire imaging area. Dashed red lines indicate the occurrence of interictal spikes. (**B**) Same as (**D**) for GCaMP6. (**C**) Distribution of the percentage of detected cells that were active during interictal spikes (stratum pyramidale median = 0.6 %, $n = 29$ interictal spikes from six mice; stratum oriens median = 33.3%, $n = 33$ interictal spikes from six mice; statistically different: two-sample Kolmogorov-Smirnov test, $P << 0.001$). (**D**) Images of the average GCaMP signal in the stratum pyramidale (*left*) and stratum oriens (*right*) corresponding to the contours of cells depicted in (**E**). Scale bars = 50 μm. (**E**) Contours of imaged cells in a single movie from the stratum pyramidale (upper, $n = 827$ cells) and stratum oriens (lower, $n = 9$ cells). Blue contours in the stratum pyramidale indicate cells that were active outside of interictal spikes. Red filled contours indicate cells recruited during a single interictal spike, and data are shown for four consecutive interictal spikes. Scale bars = 50 μm.

Table 1 Cellular recruitment during interictal spikes

	Stratum pyramidale	Stratum oriens
Number of imaged cells	766 ± 47	7 ± 1
Number of cells recruited in interictal spikes	3.7 ± 0.7	2.1 ± 0.3
Percentage of imaged cells recruited in interictal spikes	0.5 ± 0.1%	38.6 ± 4.0%
Number of active cells (outside interictal spikes)	38 ± 10	
Percentage of active cells (outside interictal spikes)	4.7 ± 1.1%	
Percentage of active cells recruited in interictal spikes	19.5 ± 3.8%	

cellular participation of cells in the stratum pyramidale combined with the supralinear relationship between the contralateral EEG amplitude and calcium response, which was independent of imaging location, this leaves GABAergic perisomatic innervation as a likely candidate for the observed diffuse increase in GCaMP fluorescence in the stratum pyramidale.

GABAergic neurons are the main participants in interictal spikes in CA1

To further test whether GABAergic cells are the main contributors to the GCaMP fluorescence signal associated with interictal spikes, we next performed imaging in TLE GAD67-Cre mice injected with a viral vector carrying a CRE dependent version of GCaMP5G (Tolu *et al.*, 2010). Here, the calcium reporter is only expressed in GABAergic cells, and the associated fluorescence signal originates solely from GABAergic neurons. GCaMP5G could be detected in the soma and dendrites, as well as in putative perisomatic axonal terminals located in the stratum pyramidale (Fig. 4A). As observed in wild-type TLE mice, interictal spikes in both the stratum pyramidale and stratum oriens were associated with transient increases in the GCaMP signal (Fig. 4B, Supplementary Videos 4 and 5, $n = 1223$ spikes from four mice). The spatial imprint of interictal spikes imaged in the stratum pyramidale clearly indicated the activation of GABAergic processes throughout the pyramidal layer (Fig. 4C), and events in the stratum oriens were confirmed to originate from the activation of a subset of cell bodies from GABAergic neurons and a web of putative dendritic processes (Fig. 4D). Importantly, we also observed the same supralinear correlation between the amplitude of the recorded contralateral EEG spike and the amplitude of the corresponding change in GCaMP fluorescence under these conditions where only GABAergic cells contributed to the GCaMP signal (Fig. 4C, Functional Data Analysis, non-parametric permutation test, no difference between groups, $P = 0.54$). Thus, the observed calcium response is the same with or without the inclusion of signals from the glutamatergic population, confirming that in CA1, the fluorescence increase during interictal spikes is driven by the activation of GABAergic cells.

Spatial patterning of local recruitment varies between interictal spikes and follows macro-scale variable dynamics

Given that GABAergic inhibition was previously identified as a possible circuit mechanism for the variable paths by which synchronous activity spreads through epileptic networks (Sabolek *et al.*, 2012), we asked whether a related variability in the recruitment of GABAergic microcircuits could be observed *in vivo*. We therefore developed an analysis to compare the spatial similarity of interictal spikes imaged in GAD67-Cre mice (Fig. 5). A similarity matrix of the spatial overlap between interictal spikes was run through a hierarchical clustering algorithm to group events with similar spatial patterning (Fig. 5A–D and Supplementary material). Matrices were resorted with respect to the results of the clustering algorithm and visually inspected for the appearance of communities (i.e. groups of neurons with similar firing patterns within the group but different from those outside the group, and visible as block-like structures along the diagonal of the sorted similarity matrix). Clear community structure was visible in the similarity matrix in five of eight analysed imaging sessions (coloured boxes in Fig. 5D), indicating that interictal spikes within a community had the same spatial structure, but that this structure was different for interictal spikes between communities, and that sequential spikes do not necessarily recruit the same population of GABAergic neurons (Fig. 5C). Therefore, we conclude that variable subpopulations of GABAergic cells compose the specific microcircuitry activated during interictal spikes in CA1.

Finally, we investigated whether this variable circuitry contributed to an observed variance in the globally recorded contralateral EEG signal. We observed a small but significant correlation (Pearson's $r = 0.13$, $P = 0.005$) between interictal spikes with correlated contralateral EEG signals and overlapping spatial imprints (Fig. 5F). Spikes with a low correlation of contralateral EEG signals were unlikely to show high spatial overlap, but the results were more variable for spikes with higher correlations between contralateral EEG signals. Some of this ambiguity could be due to the difficulty in assessing similarity when taking into account the fine dendritic structure in spatial imprints, and further work should investigate how specific GABAergic cell populations shape the electrophysiological correlates of interictal events. Regardless, this analysis demonstrates that the local variability in microcircuit recruitment reflected in the spatial patterning of calcium signals

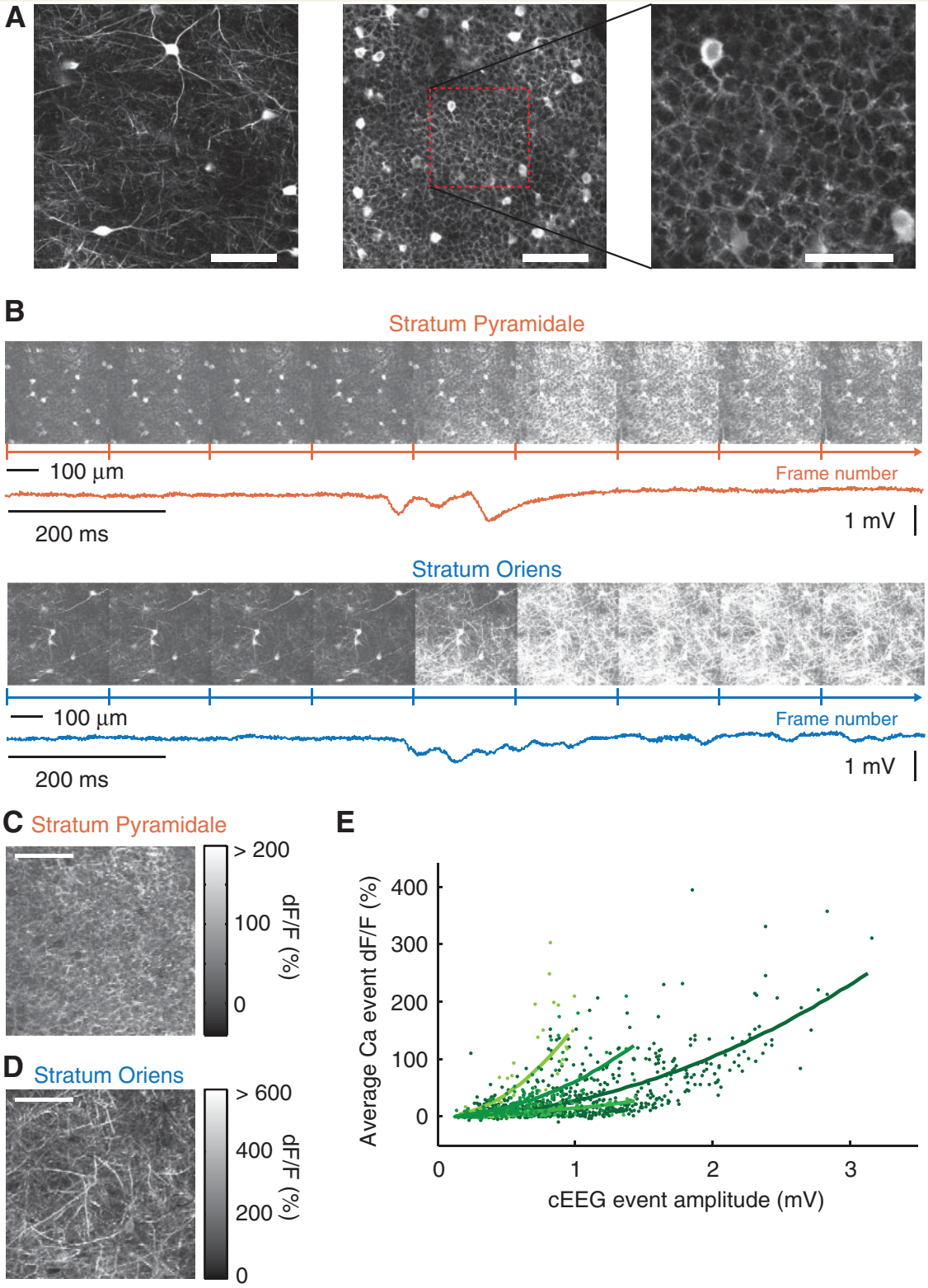

Figure 4 Calcium imaging of CA1 GABAergic neuron activity in GAD67-Cre mice. (**A**) Image of GCaMP5 signal in GABAergic cells from the stratum oriens (*left*, Scale bar = 100 µm) and stratum pyramidale (*middle*, Scale bar = 100 µm; *right*, Scale bar = 50 µm). (**B**) Successive movie frames showing GCaMP fluorescence signal from GABAergic cells and corresponding contralateral EEG signal for an interictal spike spike in the stratum pyramidale (orange, Supplementary Video 4) and stratum oriens (blue, Supplementary Video 5). (**C** and **D**) Corresponding spatial imprint of recruitment of GABAergic neurons during an interictal spike in the stratum pyramidale (**C**) and stratum oriens (**D**). Scale bar = 100 µm. (**E**) Relationship between the amplitude of the contralateral EEG and the average image dF/F during interictal spikes (same as Fig. 2D for wild-type mice, n = 4 mice, 1223 interictal spikes). Data from the stratum pyramidale and stratum oriens are pooled as the relationship was independent of the imaging location.

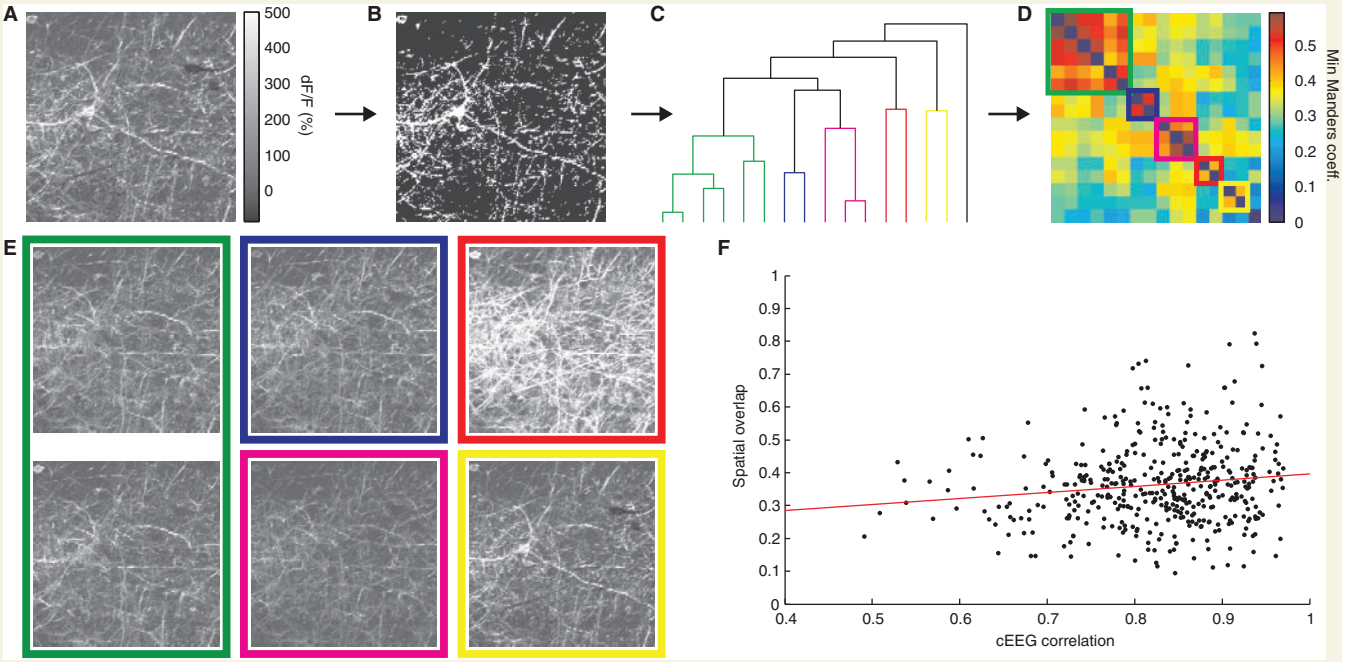

Figure 5 Spatial structure of GABAergic neuron recruitment. (**A**) Spatial imprint of an interictal spike imaged in the stratum oriens in a GAD67-Cre mouse. (**B**) Binarized version of the interictal spike in **A** showing spatial pattern of activated pixels. (**C**) Dendrogram resulting from average linkage hierarchical clustering of the similarity matrix between the spatial patterns of 16 interictal spikes from a single imaging session. (**D**) Similarity matrix sorted by the ordering from (**C**). Coloured boxes indicate observed community structure. (**E**) Examples of spatial imprints from the same community with similar spatial patterns (green) and interictal spikes with different patterns (from different communities; other coloured boxes). (**F**) Correlation between events with similar contralateral EEG during event and similar spatial structure (Pearson's r = 0.13, $P = 0.005$, $n = 436$ interictal spikes from four mice).

originating from GABAergic neurons shapes the macroscale epileptiform dynamics recorded globally.

Discussion

Here, for the first time, using two-photon calcium imaging in awake epileptic mice to probe CA1 multi-neuron dynamics with single-cell and axonal innervation resolution, we have shown that spontaneous interictal spikes recruit variable subsets of GABAergic neurons. In turn, their glutamatergic counterparts receive synchronous inhibitory input resulting from the activation of perisomatic GABAergic terminals, which reduces their firing rate, as revealed by the combined analysis of imaging and kCSD data. These results confirm previously reported increases of GABAergic transmission in various models of epilepsy (Chen *et al.*, 2001; Cossart *et al.*, 2001; Klaassen *et al.*, 2006) and theoretical predictions (Li *et al.*, 2008). Given that GABAergic neurons are a major substrate for cognitive function (Lewis, 2014), such imbalanced recruitment of inhibitory circuits, even outside of epileptogenic regions, could support the transitory or long-term cognitive impairments associated with interictal spiking (Binnie, 2003; Mosbah *et al.*, 2014). Future work should further investigate these potential links between GABAergic activation and cognitive deficits observed during interictal spiking.

Relationship to previous studies and clinical relevance

Synchronous GABAergic activity associated with epileptiform discharges has been previously reported in electrophysiological recordings from rodent acute slice models (Velazquez and Carlen, 1999; Zhang *et al.*, 2012), *in vivo* animal models (Prince, 1968), and resected human tissue (Cohen *et al.*, 2002; Huberfeld *et al.*, 2011). However, these previous studies involved reduced preparations that do not preserve network integrity and/or relied on convulsive agents (4-AP, low Mg^{2+}, high potassium, etc.) to artificially boost activity through a non-specific increase in neuronal excitability. Importantly, some of these agents (such as penicillin) have a direct action on GABAergic transmission which will likely impact cellular dynamics. In addition, previous studies analysed interictal-like events originating from normal functioning networks rather than from structurally and functionally rewired networks following epileptogenesis. The chronic experimental model studied here mimics the structural network changes reported in human patients after epileptogenesis (Curia *et al.*, 2008) and therefore is more likely to capture the relevant cellular mechanisms at the basis of epileptiform activity. The clinical translation of the synchronous activation of CA1 GABAergic neurons and resultant inhibition of principle cells observed here supports the hypothesis that

some interictal spikes in human patients may reflect a protective phenomenon (Avoli *et al.*, 2013).

In studies that have previously described an increase in inhibitory drive, this increase was generally followed or paralleled by an increase in the excitatory drive, sometimes resulting from a direct depolarizing action of GABA in pathological tissue (Cohen *et al.*, 2002). However, we do not observe this phenomenon because the activation of somatic GABAergic terminals does not induce spiking. We cannot exclude the possibility that glutamatergic activity is also contributing to the observed interictal spikes, but we do show that the synaptic inputs that potentially drive GABAergic neurons are not likely to originate from a burst of action potentials generated at the soma of local glutamatergic neurons since these neurons become quiescent during interictal spikes (although see 'Technical considerations' section below). In contrast, bursting activity is observed in principal layer neurons outside of interictal spikes, for example when the mouse is running on the treadmill.

We also provided the first *in vivo* demonstration with cellular resolution of the variability in neuronal recruitment during interictal events, a feature previously observed in slice recordings (Sabolek *et al.*, 2012; Feldt Muldoon *et al.*, 2013). Interestingly, both variability in neuronal recruitment as well as an increase in the inhibitory drive were also shown to be characteristic features of the so-called 'ictal penumbra' (Prince and Wilder, 1967; Dichter and Spencer, 1969*a*, *b*; Trevelyan *et al.*, 2006; Trevelyan, 2009; Sabolek *et al.*, 2012; Schevon *et al.*, 2012; Trevelyan and Schevon, 2013), a region around the territory supporting ictal activity that displays large amplitude EEG signals, reflecting feedforward synaptic currents, but with little actual local recruitment of neurons. The presence of an ictal penumbra suggests heterogeneity in neuronal activation with massive activation only at certain spatially focused sites. It is possible that our data reflect a similar phenomenon, however, the previous work studying penumbral regions was done in regard to ictal events and the interictal spikes observed here are very likely to involve different mechanisms of neuronal recruitment than those which lead to seizures.

This finding also has potential implications regarding the interpretation of functional MRI data obtained from epileptic patients. It is likely that the magnitude of the contribution of GABAergic neurons to the blood oxygen level-dependent signal differs from that of excitatory cells (Buzsaki *et al.*, 2007), and therefore one must be cautious when drawing conclusions about epileptiform activity when using this standard modality.

Technical considerations

As this study pushes current *in vivo* imaging techniques to their experimental limits, it is important to take some technical considerations into account when interpreting the data. First, to image at the depth of the dorsal hippocampus, it was necessary to remove a small portion of the overlying neocortex. While this could affect the propagation of interictal spikes through the neocortex, it is important to note that the interictal spikes detected in the contralateral EEG signal showed similar properties to those from previously studied TLE mice chronically implanted with a telemetric surface EEG (Feldt Muldoon *et al.*, 2013). Additionally, the linear probe experiments presented here did not involve the removal of the neocortex, and we observed the same variation in spike shape, along with a silencing of neuronal activity in the stratum pyramidale and a current source that could represent the synchronous inflow of chloride into somata resulting from synchronous GABAergic inputs. Thus, the findings from the linear probe experiments in which the cortex was not removed are consistent with the data obtained in the imaging experiments that did involve the removal of a small portion of the cortex, supporting the notion that the removal of the cortex did not greatly influence the propagation dynamics. We also note that the pilocarpine model used in this study is a multifocal model and we have no reason to suspect that one hemisphere would preferentially be associated with the focus of spikes. Although interictal spike detection was done on the contralateral side, for all detected spikes, the linear probe recordings confirmed the presence of an associated ipsilateral spike.

Another important consideration stems from the fact that the exact firing patterns of CA1 pyramidal cells during interictal spikes are difficult to assess. The sharp slope associated with interictal spikes in linear probe recordings meant that a short window of time centred on the interictal spike had to be excluded from multiunit analysis. Thus, to examine cellular participation of cells in the stratum pyramidale during interictal spikes, we turned to imaging of calcium dynamics using GCaMP. These reporters are particularly well suited for our experimental conditions since they reliably detect bursting dynamics and 'epileptic' neurons have been shown to display a higher bursting propensity (Yaari and Beck, 2002). In principle, the ability of the GCaMP reporters to detect the influx of calcium from a single action potential is less reliable. For this reason, we used both GCaMP 5 and 6 variants as the newer GCaMP6 has been shown to be more sensitive to the detection of single action potentials, both in pyramidal cells and in interneurons (Chen *et al.*, 2013). While we were able to detect more active cells in mice injected with GCaMP6 versus GCaMP5 (Supplementary material), these cells were observed to be active outside of interictal spikes, and the cellular recruitment in the stratum pyramidale during interictal spikes was not significantly different when using the two indicators. In addition, we have both directly and indirectly demonstrated the sensitivity of the GCaMP reporters to detect single spikes by performing juxtacellular spike recordings from single imaged neurons in anaesthetized mice, and by imaging ripple events in the stratum pyramidale. Still, it is possible that we failed to observe the activation of some cells in the stratum

pyramidale, especially those that display a tonic mode of firing for which two consecutive spikes are below our temporal resolution or cells that fire only a single action potential during the interictal spike.

Finally, it should be noted that we attempted to isolate the calcium signal originating only from pyramidal cells by performing calcium imaging, but could not find experimental conditions for which GCaMP expression was strictly restricted to glutamatergic neurons, as a small percentage of GABAergic cells additionally expressed the GCaMP indicator when using a CAMKII-Cre viral vector, and Emx1-Cre mice could no longer drive Cre expression in CA1 at adult stages.

Circuit mechanisms for the initiation and propagation of GABAergic activity

From a circuits perspective, our study introduces many questions. What are the upstream cellular mechanisms that support the preferential recruitment of GABAergic neurons? Are specific GABAergic microcircuits activated that contribute to the control of downstream neuronal populations? As mentioned above, the somata of most neurons located in the principal cell layer do not display spontaneous calcium transients during interictal spikes, but instead show decreased spiking as observed in multiunit extracellular recordings. It is therefore unlikely that GABAergic neurons are synaptically activated from local CA1 collateral inputs. However, it was previously reported that CA1 GABAergic neurons that were spared in the course of epileptogenesis (including those with perisomatic projections) received an enhanced glutamatergic drive that contributed to increased spontaneous firing (Cossart *et al.*, 2001). It was thought that this enhanced glutamatergic drive originated from the sprouting of local CA1 axon collaterals (Esclapez *et al.*, 1999; Cossart *et al.*, 2001). However, it may instead be that this arises from CA3 or the entorhinal cortex, as both regions provide a main excitatory drive to CA1 and were shown to be potential sites of origin for epileptiform events (Wozny *et al.*, 2005). In fact, rather than Schaffer collaterals from CA3, inputs originating from the entorhinal cortex were recently shown to be more likely to drive CA1 interneurons (as opposed to their glutamatergic counterparts) (Sun *et al.*, 2014). Additionally, it could be that glutamate is released due to distal axonal firing that occurs independently from somatic activity (Dugladze *et al.*, 2012). Alternatively, CA1 GABAergic neurons could be driven by a very sparse and currently unidentified population of glutamatergic bursting neurons (Miles and Wong, 1983; Marissal *et al.*, 2012), so we cannot exclude that GABAergic neurons could be driven by the few cells in the stratum pyramidale that are detected as being active during interictal spikes. Finally, the preferential activation of interneurons may result from several other factors, including a lower action potential threshold, short response latency, and fast axonal signalling (Geiger *et al.*, 1997; Galarreta and Hestrin, 2001; Hu *et al.*, 2010; Hu and Jonas, 2014), the properties and distribution of the excitatory synapses they receive (in particular higher amplitude excitatory postsynaptic potentials) (Gulyas *et al.*, 1999; Megias *et al.*, 2001; Molnar *et al.*, 2008), or their forming a gap-junction syncytium (Galarreta and Hestrin, 1999; Gigout *et al.*, 2006). Thus, future work is needed to identify the upstream source of GABAergic cell coordination.

Identification of the specific downstream targets of GABAergic neurons recruited during interictal spikes is also an important issue due to the critical role that subsets of GABAergic neurons play in single-handedly priming network bursts and behaviour (Bonifazi *et al.*, 2009; Ellender *et al.*, 2010; Doron *et al.*, 2014), and the fact that there is increasing experimental evidence indicating that inhibition can balance and even oppose spreading excitatory activity very effectively (Prince and Wilder, 1967; Grenier *et al.*, 2001, 2003; Timofeev *et al.*, 2002; Trevelyan *et al.*, 2006; Rheims *et al.*, 2008). Given that the cellular recruitment we describe is heterogeneous, it is likely that, in addition to perisomatic projecting neurons, other classes of GABAergic neurons are also recruited during interictal spikes. For example, the activation of somata in the pyramidal layer could be observed when imaging GAD67-Cre mice, which suggests that GABAergic neurons in that layer, i.e. basket cells and Ivy cells (Fuentealba *et al.*, 2008), could be recruited. In fact they represent a similar fraction to the fraction cells detected as being active in the stratum pyramidale during interictal spikes (Supplementary Fig. 2). Interestingly, an additional sprouting of GABAergic axons has recently been revealed, which could also link CA1 to the dentate gyrus and have important functional consequences in the present context (Peng *et al.*, 2013).

Linking micro and macroscopic scales

Finally, it is important to understand the relationship between micro and macro network activity because the various mechanisms proposed to underlie the generation of epileptiform discharges are united by the assumption that their dynamics are conserved across multiple scales. A somewhat unexpected finding of this study is the correlation between the maximum value of the kCSD source located in the pyramidal layer and the amplitude of interictal spikes recorded at the global/surface level from the contralateral EEG. Additionally, we found a supralinear relationship between the amplitude of the locally observed cellular GCaMP fluorescence signal and the contralateral EEG amplitude of interictal spikes. Notably, this relationship was independent of the depth of imaging. Given that we also observed variable spatial patterning as different subsets of GABAergic cells were recruited during sequential interictal spikes, it is unlikely that this supralinear response is solely due to a progressive increase in the number of cells recruited during spikes. In fact, it has been shown that the

relationship between the number of action potentials fired and the fluorescence amplitude of the GCaMP indicator is also supralinear (Akerboom *et al.*, 2012; Chen *et al.*, 2013). This suggests that the amplitude of the interictal spike, measured at the macroscopic scale, could reflect an increased firing rate of cells that are recruited in our microscopic imaging area. Whether or not this reflects a globally observed phenomenon throughout all brain regions or if the global signal is dominated by the GABAergic activity we observe locally remains an open question (Trevelyan, 2009; Bazelot *et al.*, 2010).

We also observed a small but significant relationship between interictal spikes with similar spatial patterning and spike shape, with the main observation being that spikes with a lower correlation between contralateral EEG shapes were unlikely to also have similar spatial patterning of cellular recruitment. Spikes with a high correlation of contralateral EEG shape displayed a more variable relationship between spatial patterning of interictal spikes. However, because of the difficulty in comparing images of the fine dendritic webs recruited during interictal spikes (even after movement correction of images, small shifts of a few pixels in dendritic location matter when comparing spatial patterns of recruitment), it is likely that our analysis underestimated this relationship. Therefore, future studies should additionally address cellular recruitment in different areas and how different brain regions and neuronal subpopulations differentially contribute to the globally measured EEG signals observed at the surface of the brain.

In conclusion, our finding that inhibitory GABAergic microcircuits are the main participants of interictal activity in CA1 supports recent theoretical and experimental predictions by connecting several separate pieces of previous evidence supporting the importance of GABAergic inhibition in shaping epileptiform activity. Importantly, we also provided the first demonstration of these principles in the intact brain of un-anaesthetized chronically epileptic animals, which is a modality that has not been previously explored. This work therefore provides valuable insight into the micro-scale epileptiform dynamics that underlie macro-scale subdural EEG signals, and suggests that large scale inhibition could potentially be related to some of the clinically observed cognitive deficits associated with interictal spikes.

Acknowledgements

We acknowledge the GENIE Program and the Janelia Farm Research Campus, specifically for GCAMP5G: Loren L. Looger, Ph.D., Jasper Akerboom, Ph.D., Douglas S. Kim, Ph.D and for GCAMP6m: Vivek Jayaraman, Ph.D., Rex A. Kerr, Ph.D., Douglas S. Kim, Ph.D., Loren L. Looger, Ph.D., Karel Svoboda, Ph.D. from the GENIE Project, Janelia Farm Research Campus, Howard Hughes Medical Institute. We also thank Daniel Wójcik for helpful comments and providing the Matlab code used in the kCSD analysis, Pr. Hannah Monyer for providing the GAD67-Cre mice, Pr. Daniel Dombeck for helping with the implantation of the chronic hippocampal imaging window and Drs E. Andresen and L. Gallais for designing the window for juxtacellular recordings.

Funding

We acknowledge funding from an FP7-PEOPLE-2011-IIF Marie Curie Fellowship (#301728 S.F.M.), an FP7-ERC 'GABA Networks' grant (#242842; V.V., T.T., R.C.), the Fondation pour la Recherche Medicale (R.C.), and an ERA-Net: EpiNet Grant (V.V., R.C.).

Supplementary material

Supplementary material is available at Brain online.

References

Akerboom J, Chen TW, Wardill TJ, Tian L, Marvin JS, Mutlu S, et al. Optimization of a GCaMP calcium indicator for neural activity imaging. J Neurosci 2012; 32: 13819–40.

Alvarado-Rojas C, Lehongre K, Bagdasaryan J, Bragin A, Staba R, Engel J, Jr, et al. Single-unit activities during epileptic discharges in the human hippocampal formation. Front Comput Neurosci 2013; 7: 140.

Ang CW, Carlson GC, Coulter DA. Massive and specific dysregulation of direct cortical input to the hippocampus in temporal lobe epilepsy. J Neurosci 2006; 26: 11850–6.

Avoli M, de Curtis CM. GABAergic synchronization in the limbic system and its role in the generation of epileptiform activity. Prog Neurobiol 2011; 95: 104–32.

Avoli M, de Curtis CM, Kohling R. Does interictal synchronization influence ictogenesis? Neuropharmacology 2013; 69: 37–44.

Badier JM, Chauvel P. Spatio-temporal characteristics of paroxysmal interictal events in human temporal lobe epilepsy. J Physiol Paris 1995; 89: 255–64.

Bazelot M, Dinocourt C, Cohen I, Miles R. Unitary inhibitory field potentials in the CA3 region of rat hippocampus. J Physiol 2010; 588: 2077–90.

Bernard C, Anderson A, Becker A, Poolos NP, Beck H, Johnston D. Acquired dendritic channelopathy in temporal lobe epilepsy. Science 2004; 305: 532–5.

Binnie CD. Cognitive impairment during epileptiform discharges: is it ever justifiable to treat the EEG? Lancet Neurol 2003; 2: 725–30.

Blume WT, Holloway GM, Wiebe S. Temporal epileptogenesis: localizing value of scalp and subdural interictal and ictal EEG data. Epilepsia 2001; 42: 508–14.

Bonifazi P, Goldin M, Picardo MA, Jorquera I, Cattani A, Bianconi G, et al. GABAergic hub neurons orchestrate synchrony in developing hippocampal networks. Science 2009; 326: 1419–24.

Bourien J, Bartolomei F, Bellanger JJ, Gavaret M, Chauvel P, Wendling F. A method to identify reproducible subsets of co-activated structures during interictal spikes. Application to intracerebral EEG in temporal lobe epilepsy. Clin Neurophysiol 2005; 116: 443–55.

Brooks-Kayal AR, Shumate MD, Jin H, Rikhter TY, Coulter DA. Selective changes in single cell GABA(A) receptor subunit expression and function in temporal lobe epilepsy [see comments]. Nat Med 1998; 4: 1166–72.

Buzsaki G, Anastassiou CA, Koch C. The origin of extracellular fields and currents–EEG, ECoG, LFP and spikes. Nat Rev Neurosci 2012; 13: 407–20.

Buzsaki G, Hsu M, Slamka C, Gage FH, Horvath Z. Emergence and propagation of interictal spikes in the subcortically denervated hippocampus. Hippocampus 1991; 1: 163–80.

Buzsaki G, Kaila K, Raichle M. Inhibition and brain work. Neuron 2007; 56: 771–83.

Cavalheiro EA, Santos NF, Priel MR. The pilocarpine model of epilepsy in mice. Epilepsia 1996; 37: 1015–19.

Chagnac-Amitai Y, Connors BW. Horizontal spread of synchronized activity in neocortex and its control by GABA-mediated inhibition. J Neurophysiol 1989; 61: 747–58.

Chauviere L, Doublet T, Ghestem A, Siyoucef SS, Wendling F, Huys R, et al. Changes in interictal spike features precede the onset of temporal lobe epilepsy. Ann Neurol 2012; 71: 805–14.

Chen K, Aradi I, Thon N, Eghbal-Ahmadi M, Baram TZ, Soltesz I. Persistently modified h-channels after complex febrile seizures convert the seizure-induced enhancement of inhibition to hyperexcitability. Nat Med 2001; 7: 331–37.

Chen TW, Wardill TJ, Sun Y, Pulver SR, Renninger SL, Baohan A, et al. Ultrasensitive fluorescent proteins for imaging neuronal activity. Nature 2013; 499: 295–300.

Cohen I, Navarro V, Clemenceau S, Baulac M, Miles R. On the origin of interictal activity in human temporal lobe epilepsy *in vitro*. Science 2002; 298: 1418–21.

Cossart R, Bernard C, Ben-Ari Y. Multiple facets of GABAergic neurons and synapses: multiple fates of GABA signalling in epilepsies. Trends Neurosci 2005; 28: 108–15.

Cossart R, Dinocourt C, Hirsch JC, Merchan-Perez A, De Felipe J, Ben-Ari Y, et al. Dendritic but not somatic GABAergic inhibition is decreased in experimental epilepsy. Nat Neurosci 2001; 4: 52–62.

Csicsvari J, Hirase H, Czurko A, Mamiya A, Buzsaki G. Fast network oscillations in the hippocampal CA1 region of the behaving rat. J Neurosci 1999; 19: RC20.

Curia G, Longo D, Biagini G, Jones RS, Avoli M. The pilocarpine model of temporal lobe epilepsy. J Neurosci Methods 2008; 172: 143–57.

de Curtis M, Avanzini G. Interictal spikes in focal epileptogenesis. Prog Neurobiol 2001; 63: 541–67.

Dichter M, Spencer WA. Penicillin-induced interictal discharges from the cat hippocampus. I. Characteristics and topographical features. J Neurophysiol 1969a; 32: 649–62.

Dichter M, Spencer WA. Penicillin-induced interictal discharges from the cat hippocampus. II. Mechanisms underlying origin and restriction. J Neurophysiol 1969b; 32: 663–87.

Dombeck DA, Harvey CD, Tian L, Looger LL, Tank DW. Functional imaging of hippocampal place cells at cellular resolution during virtual navigation. Nat Neurosci 2010; 13: 1433–40.

Doron G, von HM, Schlattmann P, Houweling AR, Brecht M. Spiking irregularity and frequency modulate the behavioral report of single-neuron stimulation. Neuron 2014; 81: 653–63.

Dugladze T, Schmitz D, Whittington MA, Vida I, Gloveli T. Segregation of axonal and somatic activity during fast network oscillations. Science 2012; 336: 1458–61.

Ellender TJ, Nissen W, Colgin LL, Mann EO, Paulsen O. Priming of hippocampal population bursts by individual perisomatic-targeting interneurons. J Neurosci 2010; 30: 5979–91.

Esclapez M, Hirsch JC, Ben-Ari Y, Bernard C. Newly formed excitatory pathways provide a substrate for hyperexcitability in experimental temporal lobe epilepsy. J Comp Neurol 1999; 408: 449–60.

Fabene PF, Navarro MG, Martinello M, Martinello M, Rossi B, Merigo F, et al. A role for leukocyte-endothelial adhesion mechanisms in epilepsy. Nat Med 2008; 14: 1377–83.

Feldt Muldoon S, Soltesz I, Cossart R. Spatially clustered neuronal assemblies comprise the microstructure of synchrony in chronically epileptic networks. Proc Natl Acad Sci USA 2013; 110: 3567–72.

Fuentealba P, Begum R, Capogna M, Jinno S, Márton LF, Csicsvari J, et al. Ivy cells: a population of nitric-oxide-producing, slow-spiking GABAergic neurons and their involvement in hippocampal network activity. Neuron 2008; 57: 917–29.

Galarreta M, Hestrin S. A network of fast-spiking cells in the neocortex connected by electrical synapses. Nature 1999; 402: 72–5.

Galarreta M, Hestrin S. Electrical synapses between GABA-releasing interneurons. Nat Rev Neurosci 2001; 2: 425–33.

Geiger JR, Lubke J, Roth A, Frotscher M, Jonas P. Submillisecond AMPA receptor-mediated signaling at a principal neuron- interneuron synapse. Neuron 1997; 18: 1009–23.

Gibbs FA, Davis H, Lennox WG. The electroencephalogram in epilepsy and conditions with impaired consciousness. Arch Neurol Psychiatry 1935; 34: 1133–48.

Gigout S, Louvel J, Kawasaki H, D'Antuono M, Armand V, Kurcewicz I, et al. Effects of gap junction blockers on human neocortical synchronization. Neurobiol Dis 2006; 22: 496–508.

Greenberg DS, Houweling AR, Kerr JN. Population imaging of ongoing neuronal activity in the visual cortex of awake rats. Nat Neurosci 2008; 11: 749–51.

Grenier F, Timofeev I, Steriade M. Focal synchronization of ripples (80-200 Hz) in neocortex and their neuronal correlates. J Neurophysiol 2001; 86: 1884–98.

Grenier F, Timofeev I, Steriade M. Neocortical very fast oscillations (ripples, 80-200 Hz) during seizures: intracellular correlates. J Neurophysiol 2003; 89: 841–52.

Gulyas AI, Freund TT. Generation of physiological and pathological high frequency oscillations: the role of perisomatic inhibition in sharp-wave ripple and interictal spike generation. Curr Opin Neurobiol 2014; 31C: 26–32.

Gulyas AI, Megias M, Emri Z, Freund TF. Total number and ratio of excitatory and inhibitory synapses converging onto single interneurons of different types in the CA1 area of the rat hippocampus. J Neurosci 1999; 19: 10082–97.

Hu H, Jonas P. A supercritical density of Na(+) channels ensures fast signaling in GABAergic interneuron axons. Nat Neurosci 2014; 17: 686–93.

Hu H, Martina M, Jonas P. Dendritic mechanisms underlying rapid synaptic activation of fast-spiking hippocampal interneurons. Science 2010; 327: 52–8.

Huberfeld G, Menendez de la PL, Pallud J, Cohen I, Le Van Quyen M, Adam C, et al. Glutamatergic pre-ictal discharges emerge at the transition to seizure in human epilepsy. Nat Neurosci 2011; 14: 627–34.

Huneau C, Benquet P, Dieuset G, Biraben A, Martin B, Wendling F. Shape features of epileptic spikes are a marker of epileptogenesis in mice. Epilepsia 2013; 54: 2219–27.

Hunt RF, Girskis KM, Rubenstein JL, Alvarez-Buylla A, Baraban SC. GABA progenitors grafted into the adult epileptic brain control seizures and abnormal behavior. Nat Neurosci 2013; 16: 692–7.

Keller CJ, Truccolo W, Gale JT, Eskandar E, Thesen T, Carlson C, et al. Heterogeneous neuronal firing patterns during interictal epileptiform discharges in the human cortex. Brain 2010; 133: 1668–81.

Klaassen A, Glykys J, Maguire J, Labarca C, Mody I, Boulter J. Seizures and enhanced cortical GABAergic inhibition in two mouse models of human autosomal dominant nocturnal frontal lobe epilepsy. Proc Natl Acad Sci USA 2006; 103: 19152–7.

Krook-Magnuson E, Armstrong C, Oijala M, Soltesz I. On-demand optogenetic control of spontaneous seizures in temporal lobe epilepsy. Nat Commun 2013; 4: 1376.

Lewis DA. Inhibitory neurons in human cortical circuits: substrate for cognitive dysfunction in schizophrenia. Curr Opin Neurobiol 2014; 26C: 22–6.

Li Y, Fleming IN, Colpan ME, Mogul DJ. Neuronal desynchronization as a trigger for seizure generation. IEEE Trans Neural Syst Rehabil Eng 2008; 16: 62–73.

Lovett-Barron M, Kaifosh P, Kheirbek MA, Danielson N, Zaremba JD, Reardon TR, et al. Dendritic inhibition in the hippocampus supports fear learning. Science 2014; 343: 857–63.

Marchionni I, Maccaferri G. Quantitative dynamics and spatial profile of perisomatic GABAergic input during epileptiform synchronization in the CA1 hippocampus. J Physiol 2009; 587: 5691–708.

Marissal T, Bonifazi P, Picardo MA, Nardou R, Petit LF, Baude A, et al. Pioneer glutamatergic cells develop into a morpho-functionally distinct population in the juvenile CA3 hippocampus. Nat Commun 2012; 3: 1316.

Megias M, Emri Z, Freund TF, Gulyas AI. Total number and distribution of inhibitory and excitatory synapses on hippocampal CA1 pyramidal cells. Neuroscience 2001; 102: 527–40.

Melzer S, Michael M, Caputi A, Eliava M, Fuchs EC, Whittington MA, et al. Long-range-projecting GABAergic neurons modulate inhibition in hippocampus and entorhinal cortex. Science 2012; 335: 1506–10.

Miles R, Wong R. Single neurons can initiate synchronized population discharge in the hippocampus. Nature 1983; 306: 371–3.

Molnar G, Olah S, Komlosi G, Füle M, Szabadics J, Varga C, et al. Complex events initiated by individual spikes in the human cerebral cortex. PLoS Biol 2008; 6: e222.

Mosbah A, Tramoni E, Guedj E, Aubert S, Daquin G, Ceccaldi M, et al. Clinical, neuropsychological, and metabolic characteristics of transient epileptic amnesia syndrome. Epilepsia 2014; 55: 699–706.

Nusser Z, Cull-Candy S, Farrant M, Hausser M, Clark BA. Differences in synaptic GABA(A) receptor number underlie variation in GABA mini amplitude Tonic synaptic inhibition modulates neuronal output pattern and spatiotemporal synaptic integration. Neuron 1997; 19: 665–78.

Peng Z, Zhang N, Wei W, Huang CS, Cetina Y, Otis TS, et al. A reorganized GABAergic circuit in a model of epilepsy: evidence from optogenetic labeling and stimulation of somatostatin interneurons. J Neurosci 2013; 33: 14392–405.

Potworowski J, Jakuczun W, Leski S, Wojcik D. Kernel current source density method. Neural Computation 2012; 24: 541–75.

Prince DA. Inhibition in "epileptic" neurons. Exp Neurol 1968; 21: 307–21.

Prince DA, Wilder BJ. Control mechanisms in cortical epileptogenic foci. "Surround" inhibition. Arch Neurol 1967; 16: 194–202.

Rheims S, Represa A, Ben-Ari Y, Zilberter Y. Layer-specific generation and propagation of seizures in slices of developing neocortex: role of excitatory GABAergic synapses. J Neurophysiol 2008; 100: 620–8.

Royer S, Zemelman BV, Losonczy A, Kim J, Chance F, Magee JC, et al. Control of timing, rate and bursts of hippocampal place cells by dendritic and somatic inhibition. Nat Neurosci 2012; 15: 769–75.

Sabolek HR, Swiercz WB, Lillis KP, Cash SS, Huberfeld G, Zhao G, et al. A candidate mechanism underlying the variance of interictal spike propagation. J Neurosci 2012; 32: 3009–21.

Schevon CA, Weiss SA, McKhann G, Jr, Goodman RR, Yuste R, Emerson RG, et al. Evidence of an inhibitory restraint of seizure activity in humans. Nat Commun 2012; 3: 1060.

Smolders I, Bortolotto ZA, Clarke VR, Warre R, Khan GM, O'Neill MJ, et al. Antagonists of GLU(K5)-containing kainate receptors prevent pilocarpine-induced limbic seizures. Nat Neurosci 2002; 5: 796–804.

Staley KJ, White A, Dudek FE. Interictal spikes: harbingers or causes of epilepsy? Neurosci Lett 2011; 497: 247–50.

Sun Y, Nguyen AQ, Nguyen JP, Le L, Saur D, Choi J, et al. Cell-type-specific circuit connectivity of hippocampal CA1 revealed through Cre-dependent rabies tracing. Cell Rep 2014; 7: 269–80.

Timofeev I, Grenier F, Steriade M. The role of chloride-dependent inhibition and the activity of fast-spiking neurons during cortical spike-wave electrographic seizures. Neuroscience 2002; 114: 1115–32.

Tolu S, Avale ME, Nakatani H, Pons S, Parnaudeau S, Tronche F, et al. A versatile system for the neuronal subtype specific expression of lentiviral vectors. FASEB J 2010; 24: 723–30.

Trevelyan AJ. The direct relationship between inhibitory currents and local field potentials. J Neurosci 2009; 29: 15299–307.

Trevelyan AJ, Schevon CA. How inhibition influences seizure propagation. Neuropharmacology 2013; 69: 45–54.

Trevelyan AJ, Sussillo D, Watson BO, Yuste R. Modular propagation of epileptiform activity: evidence for an inhibitory veto in neocortex. J Neurosci 2006; 26: 12447–55.

Truccolo W, Donoghue JA, Hochberg LR, Eskandar EN, Madsen JR, Anderson WS, et al. Single-neuron dynamics in human focal epilepsy. Nat Neurosci 2011; 14: 635–41.

Velazquez JL, Carlen PL. Synchronization of GABAergic interneuronal networks during seizure-like activity in the rat horizontal hippocampal slice. Eur J Neurosci 1999; 11: 4110–18.

Wozny C, Gabriel S, Jandova K, Schulze K, Heinemann U, Behr J. Entorhinal cortex entrains epileptiform activity in CA1 in pilocarpine-treated rats. Neurobiol Dis 2005; 19: 451–60.

Wozny C, Kivi A, Lehmann TN, Dehnicke C, Heinemann U, Behr J. Comment on "On the origin of interictal activity in human temporal lobe epilepsy *in vitro*". Science 2003; 301: 463.

Yaari Y, Beck H. "Epileptic neurons" in temporal lobe epilepsy. Brain Pathol 2002; 12: 234–9.

Zhang ZJ, Koifman J, Shin DS, Ye H, Florez CM, Zhang L, et al. Transition to seizure: ictal discharge is preceded by exhausted presynaptic GABA release in the hippocampal CA3 region. J Neurosci 2012; 32: 2499–512.

Zhou JL, Lenck-Santini PP, Zhao Q, Holmes GL. Effect of interictal spikes on single-cell firing patterns in the hippocampus. Epilepsia 2007; 48: 720–31.